RESEARCH ARTICLE

Phytate hydrolysate induces circumferential F-actin ring formation at cell–cell contacts by a Rho-associated kinase-dependent mechanism in colorectal cancer HT-29 cells

Takuya Suzuki[1,2] *and Hiroshi Hara*[1]

[1] Division of Applied Bioscience, Research Faculty of Agriculture, Hokkaido University, Japan
[2] Department of Biofunctional Science and Technology, Graduate School of Biosphere Science, Hiroshima University, Japan

Received: December 20, 2009
Revised: May 12, 2010
Accepted: May 17, 2010

Phytate (inositol hexa-phosphate or IP6) possessing anticancer activity is hydrolyzed by phytase in intestinal microbes and the metabolites are distributed throughout the colon. Cellular circumferential F-actin rings, which are involved in cell polarity and structure, are lost early during tumorigenesis. We investigated F-actin ring formation by the phytate hydrolysate in colorectal cancer HT-29 cells to explore the novel mechanisms underlying the phytate-mediated anticancer function. The phytate hydrolysate, but not inositol or phytate, induced F-actin ring formation with a peak at 10 min in the cells and was associated with phosphorylation of myosin regulatory light chain. F-actin ring formation and myosin regulatory light chain phosphorylation by the phytate hydrolysate were suppressed by inhibitors of Rho-associated kinase (ROCK), Janus kinase (JAK), c-Jun *N*-terminal kinase (JNK), and protein kinase Cδ (PKCδ). Activation of ROCK and JAK, but not JNK or PKCδ, was observed at 10 min and/or earlier after stimulation with the phytate hydrolysate. Altogether, the phytate hydrolysate induces circumferential F-actin ring formation through a ROCK-dependent myosin II activation in the HT-29 cells, which requires JAK activation and basal activities of JNK and PKC. Hydrolysis products of phytate in the intestine may contribute to anticancer function of phytate.

Keywords:
Colorectal cancer / F-actin ring / Inositol hexa-phosphate / Phytate hydrolysate
Rho-associated kinase

1 Introduction

Myo-inositol 1,2,3,4,5,6 hexa-phosphate (IP6, phytic acid or phytate) is ubiquitously distributed throughout the plant kingdom as the storage form of phosphorus in seeds. Phytate is particularly abundant in many cereal grains, oilseeds, and legumes with concentrations ranging from 0.4 to 6.4% [1]. It is reported that phytate has multiple biological functions including anticancer activity [2, 3]. Numerous animal studies have shown that dietary supplementation with phytate provides substantial protection against experimentally induced colonic cancer [4, 5]. It was reported that administration of phytate suppressed the aberrant crypt foci formation [5] and induced the cellular apoptosis [4] in rat model of colon cancer induced by azoxymethane. Furthermore, *in vitro* studies using cultured cancer cells have been conducted with phytate itself to elucidate the molecular mechanisms underlying the phytate-mediated anticancer action [6, 7]. These reports demonstrated that phytate suppressed the growth of colonic cancer cells through G1/G0 arrest and S phase inhibition [6], and induced apoptosis of the cancer cells through inhibition of the Akt/NF-κB pathway [7]. However, the precise mechanisms underlying

Correspondence: Professor Hiroshi Hara, Division of Applied Bioscience, Research Faculty of Agriculture, Hokkaido University, Kita-9, Nishi-9, Kita-ku, Sapporo 060-8589, Japan
E-mail: hara@chem.agr.hokudai.ac.jp
Fax: +81-11-706-2504

Abbreviations: IP0, inositol; **IP2,** inositol di-phosphate; **IP3,** inositol tri-phosphate; **IP3-RPH,** inositol tri-phosphate-rich phytate hydrolysate; **IP4,** inositol tetra-phosphate; **IP5,** inositol penta-phosphate; **IP6,** inositol hexa-phosphate or phytate; **JAK,** Janus kinase; **JNK,** c-Jun *N*-terminal kinase; **MLC,** myosin regulatory light chain; **MLCK,** myosin light chain kinase; **MYPT,** myosin phosphatase target subunit; **PKC,** protein kinase C; **PLC,** phospholipase C; **pMLC,** phospho-myosin regulatory light chain; **pMYPT,** phospho-myosin phosphatase target subunit 1; **pPKCδ,** phospho-protein kinase Cδ; **ROCK,** Rho-associated kinase

the phytate-mediated anticancer function remain poorly understood.

One of the reasons why the anticancer function of phytate has not been fully explored is the complexity of phytate metabolism. Phytate cannot be digested by the gastrointestinal digestive enzymes [8], although intrinsic phytase naturally present in cereals can partly hydrolyze phytate during the digestive process [9]. Therefore, a significant part of dietary phytate reaches to the large intestinal lumen in single-stomached animals, such as humans and rats. Once there, large intestinal microbes possessing high levels of phytase activity convert phytate to hydrolysates or metabolites, including inositol di-, tri-, tetra-, and penta-phosphates (IP2–5). It has been reported that the phosphorus in oatmeal phytate was almost completely removed while in the human adult intestine [10] and that 56% of dietary phytate was hydrolyzed in conventional rats [11]. Although phytate itself definitely exerts biological effects prior to degradation by intrinsic and microbial phytase, the contribution of the hydrolysates to the phytate-mediated biological effects should be considered. We previously reported that the phytate hydrolysate prepared using bacterial phytase, but not phytate itself, induces intracellular Ca^{2+} signaling by a Gαq protein-coupled receptor- and phospholipase C (PLC)-dependent mechanism in colorectal cancer cells [12]. Our results suggest that phytate expresses biological functions after hydrolysis and that the resultant hydrolysates contribute to the anticancer activity of phytate.

Cancer development and progression are complex processes, and one of the most important steps is the disruption of cell polarity [13]. It is known that normal epithelial cell structure and organization are lost early during tumorigenesis and the resultant unpolarized cells progress to malignant colorectal carcinoma. In normal intestinal epithelial cells, actin bundles are present in the form of a thick circumferential ring around each cell, aligned with the cell borders, and have a crucial role in the maintenance of cell polarity and structure [14, 15]. In the unpolarized colonic cancer cells, however, the actin ring at cell–cell contacts is thin or lost [13]. The actin bundles, so-called F-actin (filamentous actin), are polymerized with G-actin (globular or monomer actin). F-actin formation is typically associated with myosin II activity/contractility, which is regulated by the phosphorylation of myosin II regulatory light chain (MLC) [16]. Myosin II is localized at cell–cell contacts and myosin II contractility has a pivotal role in the formation of the circumferential F-actin ring and acquisition of a cuboidal cell shape in the intestinal epithelial cells [14, 17]. On the basis of this evidence, it appears that the maintenance and recovery of the circumferential F-actin ring and cell polarity can prevent cancer development.

In the present study, we examined the formation of the F-actin ring at cell–cell contacts by a partially hydrolyzed phytate in human colorectal cancer HT-29 cells, and we investigated the intracellular signaling pathway leading to F-actin ring formation.

2 Materials and methods

2.1 Chemicals

Cell culture reagents and supplies were purchased from Invitrogen (Carlsbad, CA). Rabbit anti-phospho-myosin regulatory light chain (pMLC), MLC, phospho-STAT-1, phospho-JNK (c-Jun *N*-terminal kinase), and phospho-protein kinase Cδ (pPKCδ) were purchased from Cell Signaling Technology (Danvers, MA). Rabbit anti-phospho-myosin phosphatase target subunit 1 (pMYPT-1, Thr 696) was purchased from Upstate (Temecula, CA). Rabbit anti-total MYPT-1 was purchased from Santa Cruz Biotechnology (San Diego, CA). Mouse anti-β-actin and HRP-conjugated anti-mouse and anti-rabbit IgG were purchased from Sigma (St. Louis, MO). ML-7 (a myosin light chain kinase (MLCK) inhibitor), Y27632 (a Rho-associated kinase (ROCK) inhibitor), and U73122 (a PLC inhibitor) were purchased from BIOMOL International (Plymouth Meeting, PA). AG490 (a Janus kinase (JAK) protein tyrosine kinase inhibitor), PP2 (a Src family of protein tyrosine kinase inhibitor), SB239063 (a p38 MAP kinase inhibitor), and SP600125 (a JNK inhibitor) were purchased from Alexis Biochemicals (San Diego, CA). U0126 (a MEK1 and 2 inhibitor), Ro-31-8425 (a PKCα/β/γ/ε inhibitor), and Rottlerin (a selective PKCδ inhibitor) were purchased from Calbiochem (San Diego, CA). YM-254890 (a Gαq protein inhibitor) was kindly donated by Astellas Pharma (Tokyo, Japan). All other chemicals were obtained from Wako Pure Chemical Industries (Osaka, Japan).

2.2 Preparation of phytate hydrolysate

Phytate hydrolysate was prepared, as described previously [12]. Briefly, 40 g of myo-inositol hexakis(dihydrogen phosphate) (phytate from rice, $C_6H_6(OPO_3H_2)_6 \cdot x\mathrm{Na}$, $x \geq 5$, Sigma) and 6 mg of phytase from *Aspergillus ficcum* (Sigma) were suspended in 200 mL of 50 mM sodium acetate, pH 5.5, and incubated at 37°C for 4 h. The resulting hydrolysate was boiled for 20 min to inactivate the phytase and cooled on ice. The hydrolysate was desalted using a packed column with a strongly acidic cation-exchange resin, Diaion PK216 (55 mm inner diameter, 550 mm long; Mitsubishi Chemical, Tokyo, Japan). The eluate obtained after concentration by rotary evaporator is referred to as IP3-rich phytate hydrolysate (IP3-RPH). The molar ratio of IP2:IP3:IP4 in IP3-RPH was found to be 1:8.6:3.6 by HPLC analysis, as described previously [12]. The chemical structure of the IP0 (inositol), IP6 (phytate), and the inositol phosphates (IP2–4) contained in the IP3-RPH are shown in Fig. 1. All preparations were appropriately aliquoted and stored at −40°C until experiments.

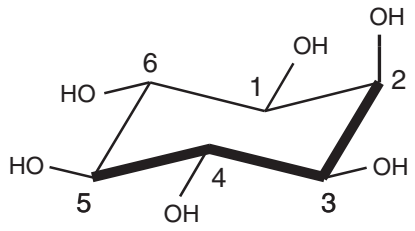

Myo-inositol

	Positions of phosphate groups
IP0 (inositol)	--
IP2	1, 2
IP3	1, 2, 6
IP4	1, 2, x, 6 (x=3, 4 or 5)
IP6 (phytate)	1, 2, 3, 4, 5, 6

Figure 1. Chemical structures of myo-inositol, phytate (IP6), and inositol phosphates in the IP3-RPH.

2.3 Cell culture

Human colorectal cancer HT-29 cells (HTB-38, American Type Culture Collection; Rockville, MD) were propagated and maintained under standard cell culture conditions, as described previously [12]. HT-29 cells were used between passages 160 and 180, and the medium was refreshed every 3 days. HT-29 cells were seeded in 24-well plates or on cover slips placed in 6-well plates at a density of 1.0×10^5 cells/cm^2. All experiments were conducted 48 h after seeding (at 50–60% confluence).

2.4 Stimulation of HT-29 cells by IP3-RPH, phytate, and inositol

HT-29 cells were washed with Hanks' balanced salt solution (134 NaCl, 4.2 $NaHCO_3$, 0.34 Na_2HPO_4,5.4 KCl, 0.44 KH_2PO_4, 1.25 $CaCl_2$, 0.49 $MgCl_2$, 0.41 $MgSO_4$, 5.6 D-glucose, 4.0 L-glutamine, and 10 HEPES (mM), pH 7.4) and bathed in 0.5 (24-well plates) or 2.0 mL (6-well plates) of Hanks' balanced salt solution. After a 30 min equilibration period, IP3-RPH (0–6.0 mM), phytate (3 mM), and inositol (3 mM) were administrated to the wells. F-actin reorganization in the cells before and at 1, 3, 10, 30, and 60 min after stimulation was visualized by immunofluorescence as described in Section 2.5. pMLC in the cells was co-stained with F-actin. Whole-cell extracts before and at 1, 3, 10, 30, and 60 min after stimulation were prepared for immunoblot analysis as described in Section 2.6.

To specify the signaling pathways involved in the IP3-RPH-mediated F-actin ring formation, the cells were loaded with the following signaling inhibitors during the equilibration period: ML-7 (an MLCK inhibitor, 30 μM), Y27632 (a ROCK inhibitor, 25 μM), BAPTA-AM (an intracellular Ca^{2+} chelator, 25 μM), YM-254890 (a Gαq protein inhibitor, 10 μM), U73122 (a PLC inhibitor, 10 μM), genistein (a non-specific protein tyrosine kinase inhibitor, 300 μM), PP2 (a Src family of protein tyrosine kinase inhibitor, 20 μM), AG490 (a JAK protein tyrosine kinase inhibitor, 50 μM), SB239063 (a p38 MAP kinase inhibitor, 10 μM), SP600125 (a JNK1/2 inhibitor, 10 μM), U0126 (a MEK1/2 inhibitor, 20 μM), Ro-31-8425 (a PKCα/β/γ/ε inhibitor, 10 μM), and Rottlerin (a PKCδ inhibitor, 10 μM). The cells were subjected to immunofluorescence or immunoblot analysis 10 min after stimulation by 3 mM IP3-RPH.

2.5 Immunofluorescence

HT-29 cells were washed with PBS, fixed with 3.7% paraformaldehyde for 10 min, and permeabilized with 0.2% Triton X-100 for 5 min. The cells were then blocked in 10% normal goat serum and 5% bovine serum albumin in PBS and incubated for 1 h with rhodamine-conjugated phalloidin to stain the F-actin. To co-stain pMLC together with F-actin, the blocked cells were incubated for 16 h at 4°C with rabbit polyclonal anti-pMLC, followed by incubation for 1 h with goat AlexaFluor 488-conjugated anti-rabbit IgG and rhodamine-conjugated phalloidin. The specimens were preserved in a mounting medium containing DAPI (ProLong®Gold Antifade Reagent, Invitrogen), and the fluorescence was visualized using a Leica FW4000 fluorescence microscope (Leica Microsystems, Germany).

2.6 Preparation of whole-cell extracts

Whole-cell extracts were prepared, as described previously [18]. Briefly, after washing with ice-cold PBS, the cells were lysed in 200 μL of lysis buffer (0.3% SDS in 10 mM Tris-containing protease inhibitors (5 μg/mL aprotinin, 3 μg/mL leupeptin hemisulfate, 5 mM benzamidine hydrochloride, and 1 mM phenylmethylsulfonyl fluoride) and phosphatase inhibitors (2 mM sodium orthovanadate and 10 mM sodium fluoride), pH 7.5). Protein concentrations in the extracts were measured by the BCA method (Pierce Biotechnology, Rockford, IL). The extracts were mixed with a half volume of Laemmli sample buffer (3 × concentrated; 6% w/v SDS, 30% v/v glycerol, 15% v/v 2-β-mercaptoethanol, and 0.02% w/v bromophenol blue in 188 mM Tris, pH 6.8) [19] and heated at 100°C for 5 min.

2.7 Immunoblot analysis

Proteins were separated by SDS-PAGE (10, 12, or 15%) and transferred to polyvinylidene difluoride membranes. Membranes were blotted for pMLC, total MLC, pMYPT-1, total MYPT-1, pSTAT-1, pJNK1/2, pPKCδ, and β-actin using

specific antibodies in combination with HRP-conjugated anti-mouse IgG or anti-rabbit IgG antibodies. The blots were developed using the ECL chemiluminescence method (GE Healthcare, Buckinghamshire, UK). Quantification was performed by densitometric analysis of specific bands on the immunoblots using Image J software.

2.8 Statistical analysis

All values are expressed as mean ± SEM. Statistical analyses were performed by one-way analysis of variance followed by Duncan's multiple range test. A difference with $p < 0.05$ was considered significant. Statistical analyses were performed using the general linear models procedure of the SAS program (version 6.07; SAS Institute).

3 Results

3.1 Induction of F-actin ring formation by IP3-RPH

To examine the effects of IP3-RPH, IP6, and IP0 on F-actin reorganization and cytoskeletal contraction, F-actin was labeled with rhodamine-conjugated phalloidin in HT-29 cells stimulated by these three compounds at 3 mM (Fig. 2). The fluorescence intensity of the labeled F-actin in cells before stimulation was weak, and F-actin was observed to be distributed broadly and loosely in the cells. The fluorescence intensity of F-actin was clearly increased at cell–cell junctions, indicating F-actin reorganization, specifically F-actin ring formation, 3 min after stimulation with IP3-RPH, and the F-actin bundles became thicker and more tightly packed at cell–cell contacts at 10 min. The F-actin ring induced by IP3-RPH was still clearly observed at 30 and 60 min, but the F-actin fluorescence intensity became weaker at these time points. Phytate and inositol did not influence the distribution or reorganization of F-actin in the cells at any time point (data not shown). No differences were found in the DAPI-stained nuclei between the cells stimulated by IP3-RPH, phytate, or inositol at any time points.

3.2 Induction of MLC phosphorylation by IP3-RPH

IP3-RPH increased MLC phosphorylation without any changes in MLC expression (Fig. 3A). The phosphorylation peaked at 10 min after stimulation with IP3-RPH and gradually decreased to the basal level at 30 or 60 min, and the pattern of the change was associated with F-actin ring formation induced by IP3-RPH (Fig. 2). The MLC phosphorylation was increased in an IP3-RPH dose-dependent manner (Fig. 3B). Densitometric analysis showed the significant increases in phosphorylation at the dose of 1 mM or higher of IP3-RPH when compared with the control value and a similar level of phosphorylation was induced by IP3-RPH at 3 and 6 mM.

Under immunofluorescence microscopy, higher fluorescence intensities for pMLC as well as for F-actin were observed in the cells at 10 min after stimulation with 3 mM IP3-RPH when compared with the those in the control cells (vehicle) (Fig. 3C). The pMLC fluorescence was weak and dispersed in the control cells. In the cells stimulated by IP3-RPH, the pMLC fluorescence was partly localized at the cell–cell contacts, where it was co-localized with phalloidin-labeled F-actin rings, suggesting that the IP3-RPH-mediated F-actin ring formation was triggered by the activation/phosphorylation of MLC. The pMLC fluorescence was also co-localized with the nuclei in the IP3-RPH-stimulated cells.

3.3 Inhibition of the IP3-RPH-mediated MLC phosphorylation and F-actin ring formation by a ROCK inhibitor

To identify the kinase responsible for the IP3-RPH-mediated MLC phosphorylation and F-actin ring formation, specific inhibitors of MLCK (ML-7) and ROCK (Y27632) were used (Fig. 4). The IP3-RPH-mediated phosphorylation of MLC was almost completely diminished by Y27632, but not by ML-7 (Fig. 4A and B). Immunofluorescence also showed that the F-actin ring formation and MLC phosphorylation induced by IP3-RPH was clearly suppressed by Y27632, but not by ML-7 (Fig. 4C).

3.4 ROCK activation by IP3-RPH

Phosphorylation of the well-known ROCK substrate MYPT-1, which indicates ROCK activity, was assessed in cells stimulated by IP3-RPH (Fig. 5). IP3-RPH transiently increased MYPT-1 phosphorylation without any change in expression (Fig. 5A). The MYPT-1 phosphorylation induced by IP3-RPH peaked at 10 min and then gradually decreased at 30 and 60 min. The increases in MYPT phosphorylation were observed in an IP3-RPH dose-dependent manner (Fig. 5B). Densitometric analysis showed that significant increases in MYPT phosphorylation at IP3-RPH concentrations of 1 mM or higher when compared with the control value, and similar increases were induced by 3 and 6 mM IP3-RPH.

3.5 Involvement of protein tyrosine kinase in the IP3-RPH-mediated MLC phosphorylation

To examine the involvement of tyrosine protein kinases and IP3-RPH-induced intracellular calcium signaling in the MLC phosphorylation induced by IP3-RPH, inhibitors of nonselective tyrosine protein kinase (genistein), Gα protein inhibitor (YM-254890), PLC (U73122), and intracellular calcium chelator (BAPTA-AM) were used (Fig. 6). The IP3-RPH-mediated MLC phosphorylation was clearly suppressed by genistein, but not by any of the other three inhibitors

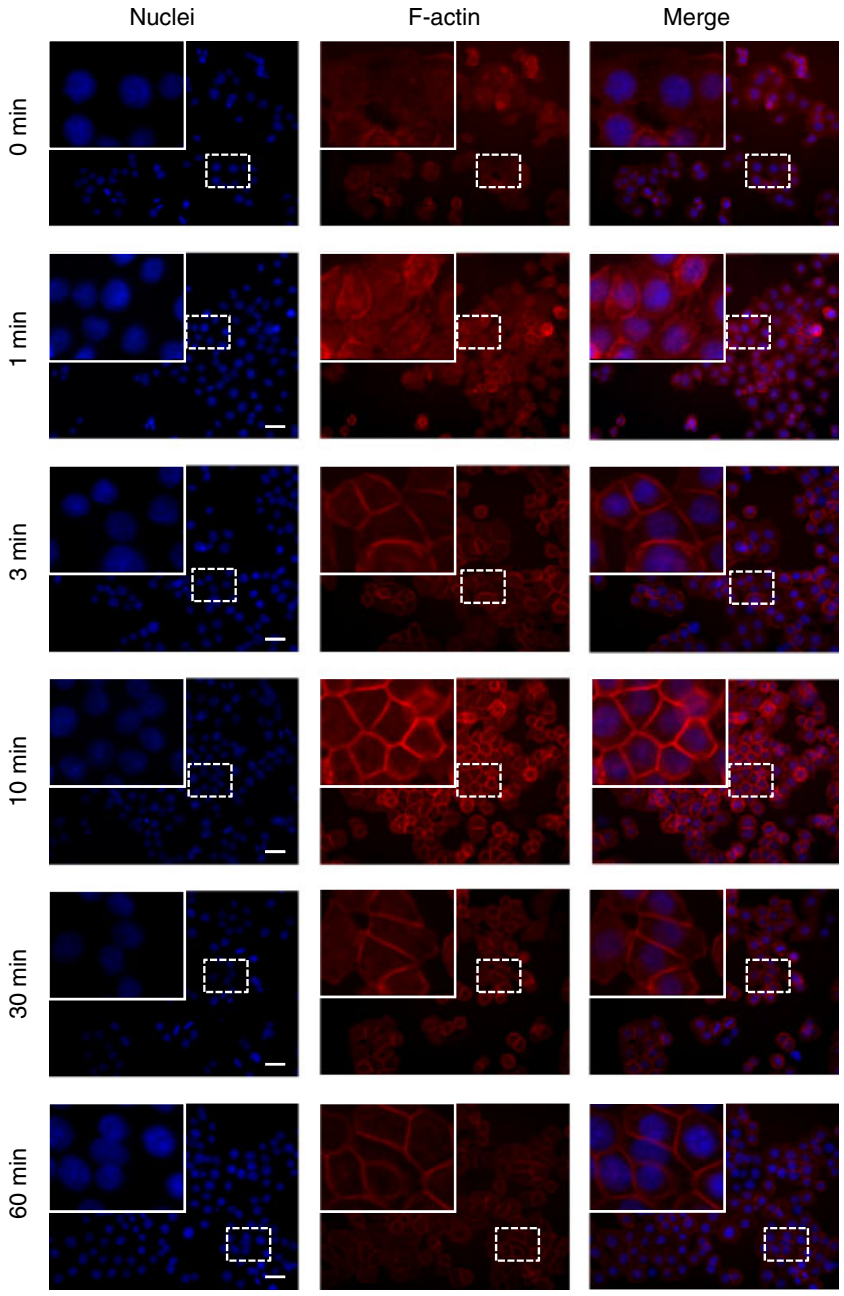

Figure 2. IP3-RPH-induced F-actin ring formation in HT-29 cells. HT-29 cells were fixed before (0 min) and at 1, 3, 10, 30, and 60 min after stimulation with IP3-RPH and stained for F-actin (red) and nuclei (blue) using an immunofluorescence method. The inset represents an enlarged view of the area enclosed within the dotted line. Each image is representative of four specimens. Images were obtained under fluorescence microscopy. Scale bars in the images represent 100 μm.

(Fig. 6A). The immunoblot analysis of phospho-tyrosine demonstrated a remarkable band of around ~90 kDa at 3 and 10 min after stimulation with IP3-RPH (Fig. 6B).

3.6 Involvements of JAK, JNK, and PKCδ in the IP3-RPH-mediated MLC phosphorylation and F-actin ring formation

The involvement of two tyrosine kinases, Src family and JAK, in the IP3-RPH-mediated MLC phosphorylation was examined (Fig. 7A). The increase in MLC phosphorylation induced by IP3-RPH was clearly suppressed by the JAK inhibitor (AG490), but not by the Src inhibitor (PP2), and the suppression was comparable to that by genistein. In addition, the participation of MAP kinase and PKC pathways in the IP3-RPH-mediated effects was investigated using the inhibitors of p38 MAP kinase (SB239063), JNK (SP600125), MEK1/2 (U0126), PKCα/β/γ/ε (Ro-31-8425), and PKCδ (Rottlerin) (Fig. 7B). The results showed that the inhibitors of JNK (SP600125) and PKCδ (Rottlerin), but not the other inhibitors, clearly suppressed the IP3-RPH-

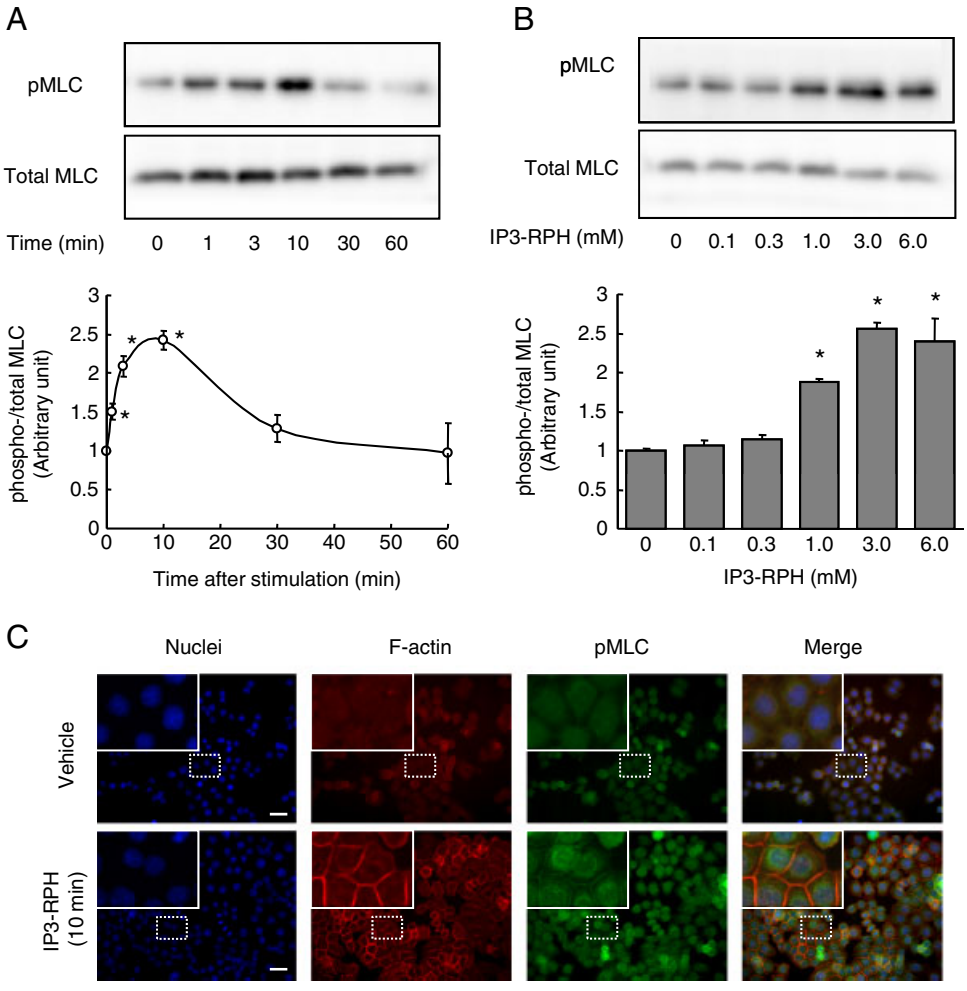

Figure 3. IP3-RPH-induced MLC phosphorylation in HT-29 cells. (A) Whole-cell extracts were prepared before (0 min) and at 1, 3, 10, 30, and 60 min after stimulation with 3 mM IP3-RPH and immunoblotted for pMLC and total MLC ($^*p<0.05$, *versus* the value before stimulation; $n=4$). (B) Whole-cell extracts were prepared at 10 min after stimulation with 0, 0.1, 0.3, 1.0, 3.0, and 6.0 mM IP3-RPH and immunoblotted for pMLC and total MLC ($^*p<0.05$, *versus* the value with 0 mM IP3-RPH; $n=4$). Each immunoblot is representative of four cell extracts. Each specific band of pMLC and total MLC was quantitated by densitometric analysis and the ratio of pMLC to total MLC was calculated. (C) HT-29 cells were fixed at 10 min after stimulation without or with IP3-RPH and stained for F-actin (red), pMLC (green), and nuclei (blue) using an immunofluorescence method. Each image is representative of four specimens. Images were obtained under fluorescence microscopy. Scale bars in the images represent 100 μm.

mediated MLC phosphorylation. Immunofluorescence microscopy revealed that the IP3-RPH-mediated increases in the fluorescence intensities of phalloidin-labeled F-actin and pMLC at the cell–cell contacts were diminished by three inhibitors, AG490, SP600125, and Rottlerin, very similarly to the immunoblot analysis of pMLC (Fig. 7C).

3.7 Activation of JAK and PKCδ, but not JNK, by the IP3-RPH

Phosphorylation of STAT-1 (a target molecule of JAK), indicating JAK activity, was transiently increased by IP3-RPH (Fig. 8A). Densitometric analysis showed that STAT-1 phosphorylation rapidly increased from 1 min after stimulation with IP3-RPH until 10 min, and then gradually decreased at 30 and 60 min. Phosphorylation of JNK1, indicating the kinase activity, was unchanged at 10 min after stimulation with IP3-RPH; however, the intensity of the specific bands of JNK1 (~46 kDa) was markedly decreased and an extra band that reacted with anti-phospho-JNK1/2 appeared at around 37 kDa at 30 and 60 min (indicated by a dagger in the Fig. 8A). JNK2 phosphorylation was not changed by stimulation with IP3-RPH at any time point. Phosphorylation of PKCδ, indicating the kinase activity, was unchanged at 10 min after stimulation with IP3-RPH, and was higher at 30 and 60 min when compared with the control value. The IP3-RPH-induced STAT-1 phosphorylation was completely blocked by the JAK inhibitor (AG490), but not by the JNK (SP600125) or PKCδ (Rottlerin) inhibitors (Fig. 8B).

4 Discussion

The present study demonstrated that IP3-RPH, a phytate hydrolysate, produced by bacterial phytase induced circumferential F-actin ring formation at cell–cell contacts through ROCK-dependent myosin II activation in unpolarized colorectal HT-29 cells (Fig. 9). The ROCK activation leading to F-actin ring formation required JAK activation and basal level JNK1 and PKCδ activity. As IP0 and phytate (IP6) lack this activity, our results indicate a novel mechanism underlying phytate-mediated biological functions.

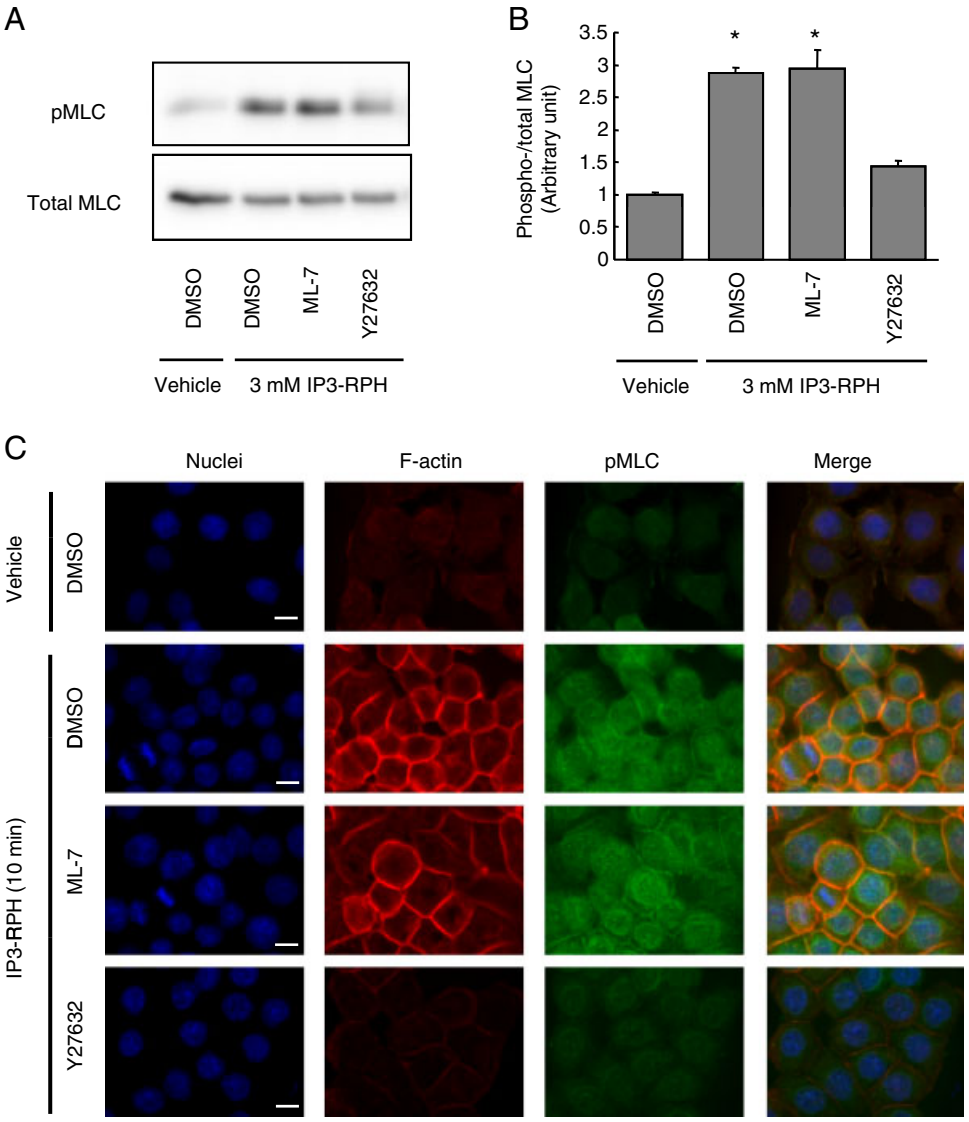

Figure 4. ROCK-dependent IP3-RPH-induced MLC phosphorylation and F-actin ring formation. (A) Whole-cell extracts were prepared at 10 min after stimulation without or with 3 mM IP3-RPH in the absence or presence of ML-7 (an MLCK inhibitor) or Y27632 (a ROCK inhibitor) and immunoblotted for pMLC and total MLC. Each immunoblot is representative of four cell extracts. Each specific band of pMLC and total MLC were quantitated by densitometric analysis and the ratio of pMLC to total MLC was calculated ($^*p < 0.05$, *versus* the value without IP3-RPH; $n = 4$). (C) HT-29 cells were fixed at 10 min after stimulation without or with 3 mM IP3-RPH in the absence or presence of ML-7 (an MLCK inhibitor) or Y27632 (a ROCK inhibitor) and stained for F-actin (red), pMLC (green), and nuclei (blue) using an immunofluorescence method. Each image is representative of four specimens. Images were obtained under fluorescence microscopy. Scale bars in the images represent 40 μm.

We first examined the effects of inositol, phytate, and IP3-RPH on F-actin reorganization and found that only IP3-RPH, but not inositol or phytate, induced F-actin ring formation in the HT-29 cells. This result clearly indicates that the F-actin ring formation does not simply depend on the presence of an inositol ring or phosphate groups in the inositol phosphates, and is associated with the combination and configuration of phosphate groups on the inositol ring. The IP3-RPH used in the study is a mixture of IP2, IP3, and IP4, with the molar ratio of IP2:IP3:IP4 being 1:8.6:3.6 according to HPLC analysis [12]. IP3 in the IP3-RPH carries phosphate groups at positions 1, 2, and 6 of the inositol ring and is a position isomer of inositol 1, 4, 5 tri-phosphate, a intracellular second messenger. IP3-RPH was prepared based on our results showing that the rank order of the potency for the induction of intracellular Ca^{2+} mobilization in HT-29 cells was IP3 > IP2 = IP4 [12]. Further studies, however, are required to identify the rank order of potency for the induction of F-actin ring formation among the inositol phosphates.

The F-actin ring formation at cell–cell contacts was found at 3 min after stimulation with IP3-RPH with a peak at 10 min, and the formed F-actin ring remained observable until 60 min. It is known that normal intestinal epithelial cells present a thick F-actin ring, which is required for the development of a column-shaped polarized cell. The F-actin ring is lost early during tumorigenesis, and those cells progress to unpolarized malignant colorectal carcinoma. Many studies using both animals and cell cultures have shown that phytate provides substantial protection against carcinogenesis and cancer development, although the precise mechanisms underlying the phytate-mediated protective effect remains poorly understood. Our results suggest that the F-actin ring formation induced by

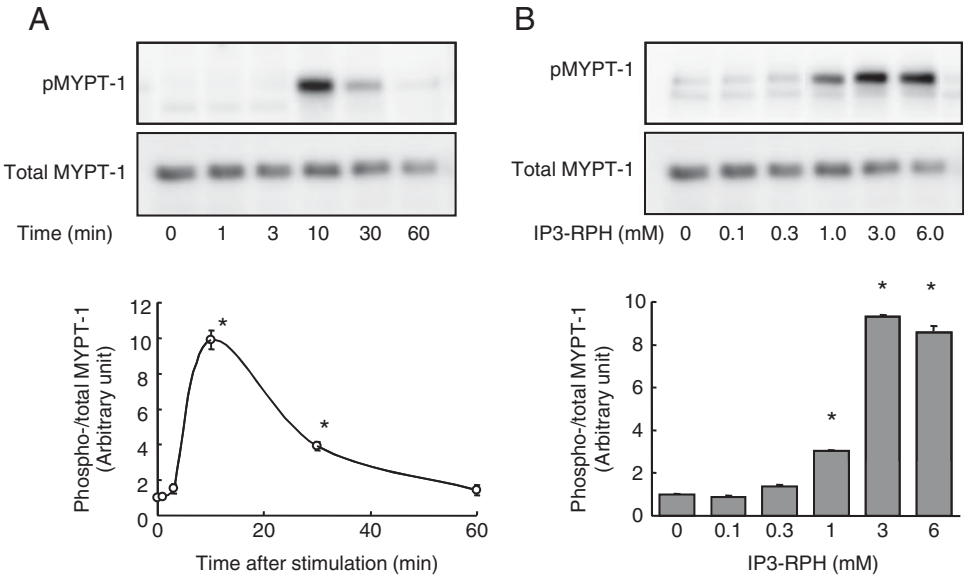

Figure 5. IP3-RPH-induced ROCK activation in HT-29 cells. (A) Whole-cell extracts were prepared before (0 min) and at 1, 3, 10, 30, and 60 min after stimulation with 3 mM IP3-RPH and immunoblotted for pMYPT-1 and total MYPT-1 ($^{*}p<0.05$, *versus* the value before stimulation; $n=4$). (B) Whole-cell extracts were prepared at 10 min after stimulation with 0, 0.1, 0.3, 1.0, 3.0, and 6.0 mM IP3-RPH and immunoblotted for pMYPT-1 and total MYPT-1 ($^{*}p<0.05$, *versus* the value with 0 mM IP3-RPH; $n=4$). Each immunoblot is representative of four cell extracts. Each specific band of pMYPT-1 and total MYPT-1 was quantitated by densitometric analysis and the ratio of pMYPT-1 to total MYPT-1 was calculated.

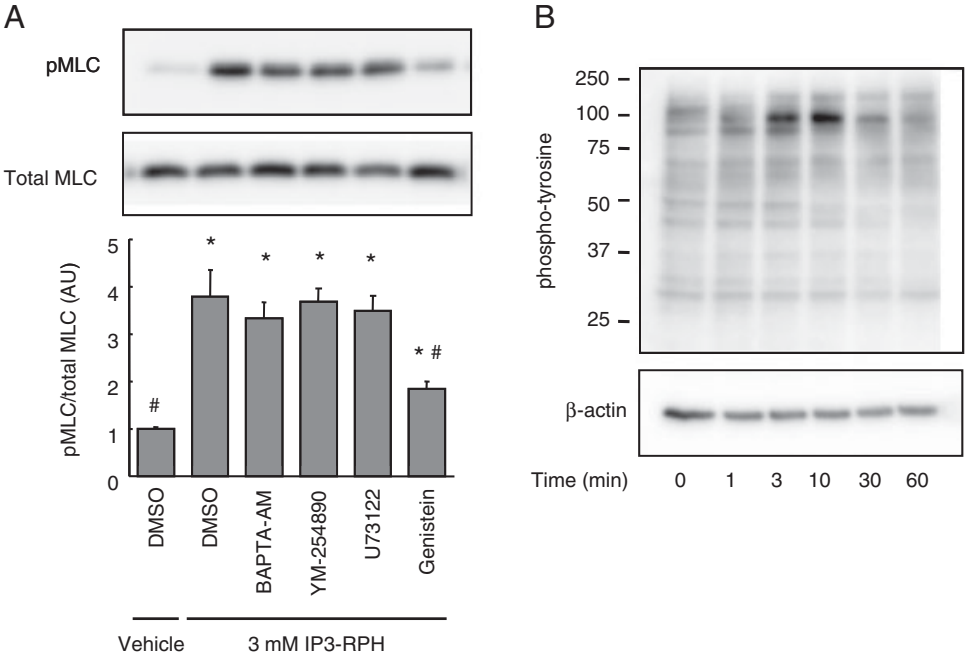

Figure 6. Protein tyrosine kinase-dependent IP3-RPH-induced MLC phosphorylation. (A) Whole-cell extracts were prepared at 10 min after stimulation without or with 3 mM IP3-RPH in the absence or presence of BAPTA-AM (an intracellular Ca^{2+} chelator), YM-254890 (a Gαq protein inhibitor), U73122 (a PLC inhibitor), or genistein (a non-specific protein tyrosine kinase inhibitor) and immunoblotted for pMLC and total MLC. Each immunoblot is representative of four cell extracts. Each specific band of pMLC and total MLC was quantitated by densitometric analysis and the ratio of pMLC to total MLC was calculated ($^{*}p<0.05$, *versus* the value before stimulation; $^{\sharp}p<0.05$, *versus* the value with IP3-RPH without inhibitors; $n=4$). (B) Whole-cell extracts were prepared before (0 min) and at 1, 3, 10, 30, and 60 min after stimulation with 3 mM IP3-RPH and immunoblotted for phospho-tyrosine. Each immunoblot is representative of four cell extracts.

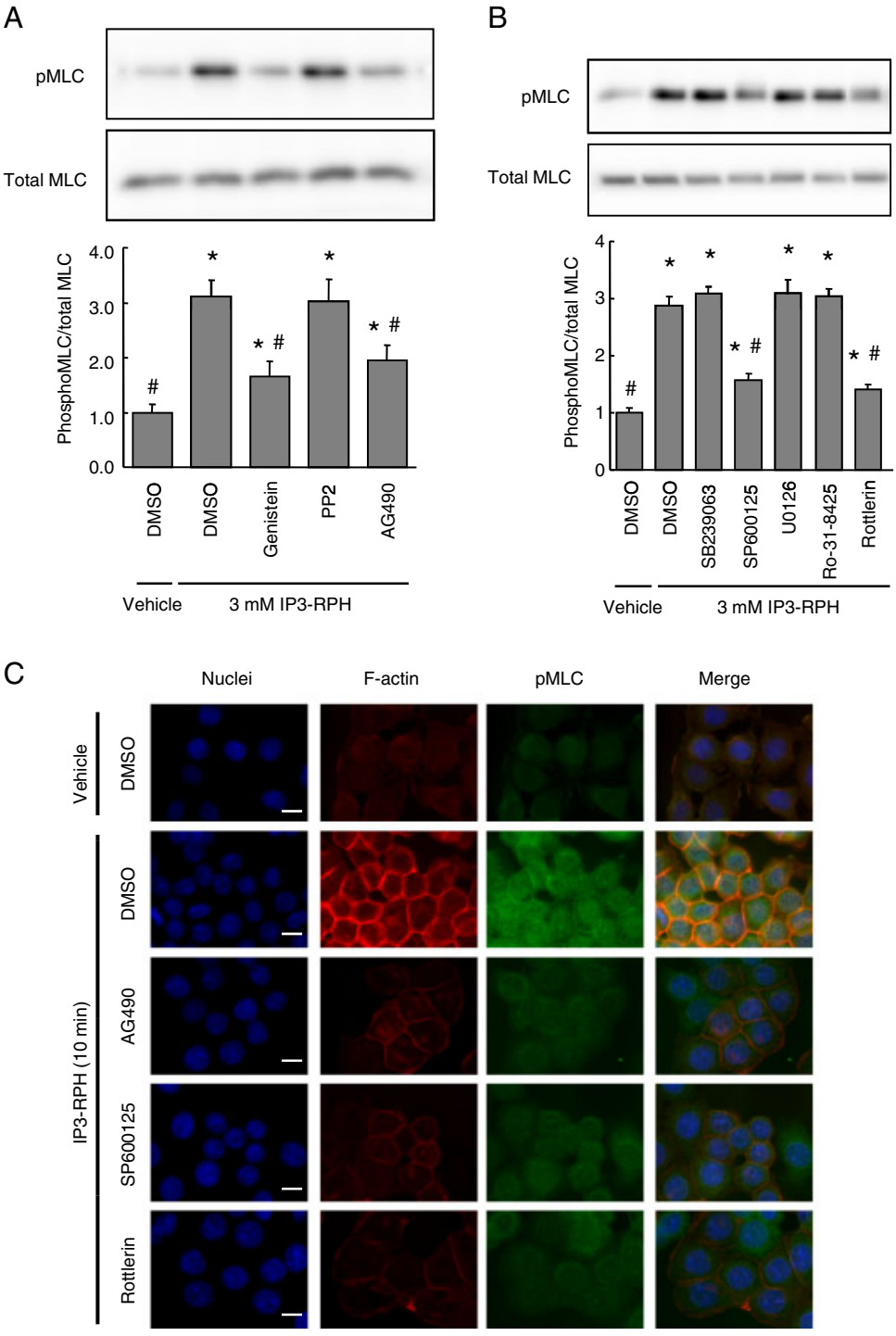

Figure 7. JAK-, JNK-, and PKCδ-dependent IP3-RPH-induced MLC phosphorylation and F-actin ring formation in HT-29 cells. (A) Whole-cell extracts were prepared at 10 min after stimulation without or with 3 mM IP3-RPH in the absence or presence of genistein (a non-specific protein tyrosine kinase inhibitor), PP2 (a Src family inhibitor), or AG490 (a JAK inhibitor) and immunoblotted for pMLC and total MLC. (B) Whole-cell extracts were prepared at 10 min after stimulation without or with 3 mM IP3-RPH in the absence or presence of SB239063 (a P38 MAP kinase inhibitor), SP600125 (a JNK1/2 inhibitor), U0126 (a MEK1/2 inhibitor), Ro-31-8425 (a PKCα/β/γ/ε inhibitor), or Rottlerin (a PKCδ inhibitor) and immunoblotted for pMLC and total MLC. Each specific band of pMLC and total MLC was quantitated by densitometric analysis and the ratio of pMLC to total MLC was calculated ($^{*}p<0.05$, *versus* the value without IP3-RPH; $^{\#}p<0.05$, *versus* the value with IP3-RPH without inhibitors; $n=4$). (C) HT-29 cells were fixed at 10 min after stimulation without or with 3 mM IP3-RPH in the absence or presence of AG490, SP600125, or Rottlerin and stained for F-actin (red), pMLC (green), and nuclei (blue) using an immunofluorescence method. Each image is representative of four specimens. Images were obtained under fluorescence microscopy. Scale bars in the images represent 40 μm.

IP3-RPH contributes to the phytate-mediated anticancer function.

Typically, the formation of diverse actin structures is associated with myosin II activity, which is regulated by MLC phosphorylation [16]. The circumferential F-actin ring formation induced by IP3-RPH was seen to be temporally associated with the MLC phosphorylation in the immunoblot analysis. Furthermore, immunofluorescence demonstrated that pMLC was partially co-localized with F-actin bundles at the cell–cell contacts in cells stimulated by IP3-RPH. To date, at least two kinases, MLCK [20] and ROCK [21], have been identified as responsible for MLC phosphorylation. A specific ROCK inhibitor (Y27632), but not the MLCK inhibitor (ML-7), clearly suppressed the

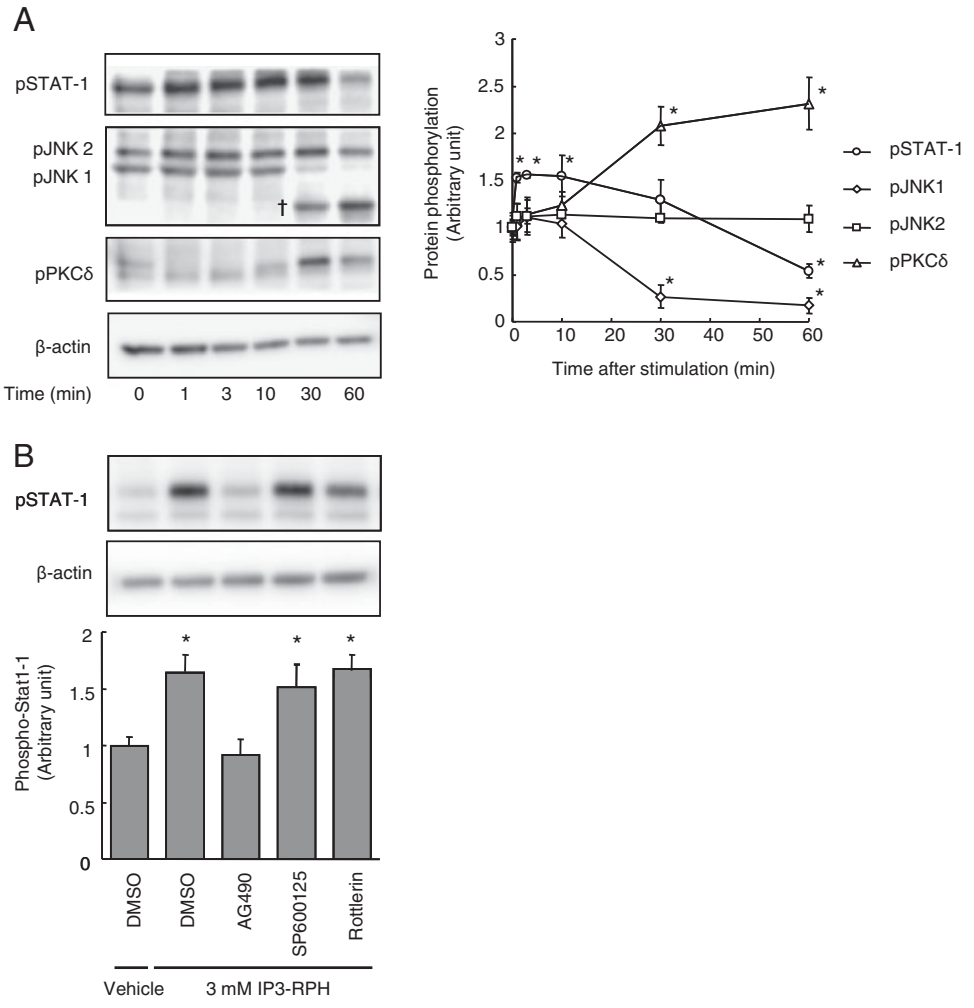

Figure 8. Phosphorylations of STAT-1, JNK1, JNK2, and PKCδ in HT-29 cells stimulated with IP3-RPH. (A) Whole-cell extracts were prepared before (0 min) and at 3, 1, 3, 10, 30, and 60 min after stimulation with 3 mM IP3-RPH and immunoblotted for pSTAT-1, pJNK1/2, pPKCδ and β-actin. Each specific band was quantitated by densitometric analysis (*$p<0.05$, *versus* the value before stimulation; $n=4$). † indicates an extra band that appeared after stimulation with IP3-RPH. (B) Whole-cell extracts were prepared at 10 min after stimulation without or with 3 mM IP3-RPH in the absence or presence of AG490 (a JAK inhibitor), SP600125 (a JNK1/2 inhibitor), or Rottlerin (a PKCδ inhibitor) and immunoblotted for pSTAT-1 and β-actin. Each specific band of pSTAT-1 was quantitated by densitometric analysis (*$p<0.05$, *versus* the value without IP3-RPH; $n=4$).

IP3-RPH-mediated MLC phosphorylation and F-actin ring formation. Furthermore, MYPT-1 phosphorylation in cells, which indicates ROCK activity, was increased, with a peak observed at 10 min after stimulation with IP3-RPH. MYPT-1 phosphorylation then gradually decreased at 30 and 60 min in association with MLC phosphorylation and F-actin ring formation. These results indicate that ROCK activation is responsible for the IP3-RPH-induced MLC phosphorylation and subsequent F-actin ring formation.

We examined the involvement of intracellular Ca^{2+} signaling in the IP3-RPH-mediated F-actin ring formation as we previously reported that the Ca^{2+} mobilization was induced by IP3-RPH through a Gαq protein-coupled receptor- and PLC-dependent mechanism in HT-29 cells [12]. However, an intracellular Ca^{2+} chelator (BAPTA-AM) and inhibitors of Gαq protein-coupled receptor (YM-254890) and PLC (U73122), all of which reduced IP3-RPH-induced Ca^{2+} mobilization [12], failed to suppress the IP3-RPH-induced MLC phosphorylation. This result means that IP3-RPH induces the F-actin ring formation independently of Ca^{2+} mobilization and that the sensory molecule for IP3-RPH leading to F-actin ring formation is different from that for the Gαq protein-coupled receptor. On the contrary, a non-specific protein tyrosine kinase inhibitor (genistein), which did not suppress IP3-RPH-induced Ca^{2+} mobilization [12], clearly attenuated the IP3-RPH-mediated MLC phosphorylation, indicating that protein tyrosine kinase(s) has a role in IP3-RPH-mediated F-actin ring formation. Moreover, immunoblot analysis revealed that protein(s) around ~90 kDa were phosphorylated on tyrosine residues at 3 and 10 min after the stimulation of cells with IP3-RPH. Therefore, we examined the involvement of two protein tyrosine kinases, Src family and JAK, in the IP3-RPH-mediated effect using their specific inhibitors. The JAK inhibitor (AG490), but not the c-Src inhibitor (PP2), suppressed the IP3-RPH-mediated MLC phosphorylation and F-actin ring formation, and the suppression was comparable to that by genistein. Immunoblot analysis showed that STAT-1 phosphorylation, which indicates JAK activity, was increased in the cells at 1, 3, and 10 min after stimulation with IP3-RPH. These results showed that IP3-RPH induced the F-actin ring formation and MLC

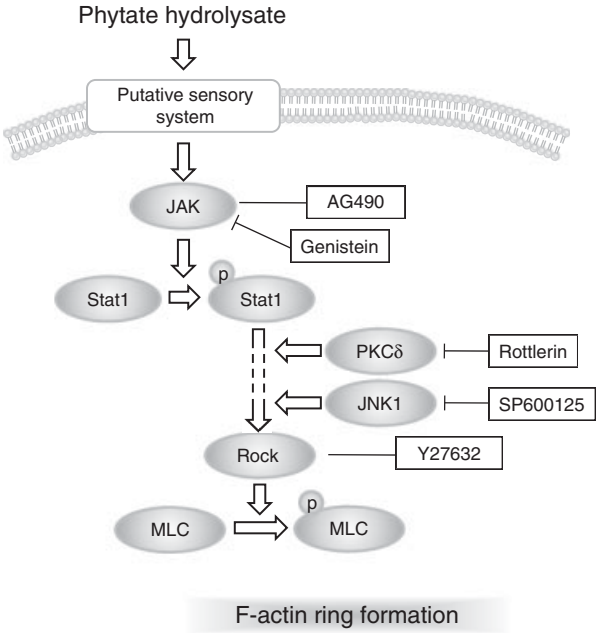

Figure 9. A diagram showing the signaling pathway leading to IP3-RPH-induced F-actin ring formation.

phosphorylation through JAK activation. The molecular weight of STAT-1 is ~91 kDa (α-isoform: 91 kDa; β-isoform: 84 kDa), and the band that appeared around ~90 kDa after IP3-RPH stimulation in the immunoblot analysis of phospho-tyrosine appears to correspond to the specific band of pSTAT-1.

We found that the JNK1/2 inhibitor (SP600125) also attenuated the IP3-RPH-mediated MLC phosphorylation and F-actin ring formation. However, IP3-RPH did not enhance JNK1/2 phosphorylation, which indicates the kinase activity, and the specific band of pJNK1 was decreased at 30 and 60 min after stimulation by IP3-RPH while an extra band of around 37 kDa was observed. The protein corresponding to the extra band seemed to be the degradation product of pJNK1, as it strongly reacted with anti-pJNK1/2. Some kinases are reported to be degraded by the ubiquitin-proteasome pathway after catalyzing phosphorylation [22]. This evidence suggests that IP3-RPH-mediated F-actin ring formation requires basal level JNK1 activity. Likewise, we suggest that basal level PKCδ activity is also required for the IP3-RPH-mediated effect. Although the PKCδ inhibitor (Rottlerin) suppressed the IP3-RPH effect, the increase in PKCδ phosphorylation (activity) by IP3-RPH was observed at 30 and 60 min after stimulation with IP3-RPH, which was later than the time at which F-actin ring formation occurred. PKCδ is generally considered to have anti-tumorigenic roles because it shows pro-apoptotic effects in many cell types [23]. It has been reported that phytate blocks proliferation of human breast cancer cells through a PKCδ-dependent increase in p27Kip1 and decrease in retinoblastoma protein phosphorylation [24]. The JNK1/2 (SP600125) and PKCδ (Rottlerin) inhibitors did not attenuate STAT-1 phosphorylation, but did suppress IP3-RPH-induced F-actin ring formation, indicating that JNK1 and PKCδ have roles in the downstream signaling pathway of JAK leading to MLC phosphorylation and F-actin ring formation.

We did not clarify how the extracellular IP3-RPH initiated the signaling pathway leading to the F-actin reorganization. Uptake and metabolism of phytate (IP6) in the cell are complex and controversial. Ferry *et al.* reported that the 2-h-pretreatment of HeLa cells with phytate blocked the cell survival pathway induced by tumor necrosis factor and insulin [7]. They suggested that the extracellular phytate was pinocytotically transported into cells, dephosphorylated partially, and inhibited the Akt/NF-κB pathway. Although the IP3-RPH could be pinocytotically transported into the cells, we would suggest that a putative sensory molecule on the plasma membrane recognizes the extracellular IP3-RPH and initiates the signaling pathway leading to the F-actin ring formation because the IP3-RPH-induced phosphorylation of MLC has been already observed just 1 min after stimulation.

The IP3-RPH at concentrations of 1 mM or higher induced the MLC phosphorylation in the cells. The information about the luminal phytate hydrolysate concentrations after a meal in humans and rodents is completely lacking, but the previous studies at least showed the fecal phytate concentration in the humans. Owen *et al.* reported that the phytate concentration was detected in the rage of 0.64–4.0 mmol/kg wet feces in patients with sporadic adenoma [25]. According to this report, the millimolar concentration of the phytate metabolites can be achievable in the colon of humans, although the daily intake of phytate varies depending on the consumption of cereals or legumes [26–28].

In conclusion, phytate hydrolysate induces the F-actin ring formation by a ROCK-dependent MLC phosphorylation in the human colorectal cancer cells. The ROCK activation occurs through the JAK, JNK, and PKCδ pathways. The phytate hydrolysate-induced F-actin ring formation may play a role in the phytate-mediated anticancer function previously observed in animals and colorectal cancer cells.

The authors express their thanks to Dr. Hiroshi Ishikawa for his cooperation in the preparation of IP3-RPH.

The authors have declared no conflict of interest.

5 References

[1] Harland, B. F., Oberleas, D., Phytate in foods. *World Rev. Nutr. Diet* 1987, *52*, 235–259.

[2] Vucenik, I., Shamsuddin, A. M., Cancer inhibition by inositol hexaphosphate (IP6) and inositol: from laboratory to clinic. *J. Nutr.* 2003, *133*, 3778S–3784S.

[3] Vucenik, I., Shamsuddin, A. M., Protection against cancer by dietary IP6 and inositol. *Nutr. Cancer* 2006, *55*, 109–125.

[4] Guido, M., Fagundes, D. J., Ynouye, C. M., Pontes, E. R. *et al.*, Apoptotic effects of inositol hexaphosphate on biomarker Itpr3 in induced colon rat carcinogenesis. *Acta Cir. Bras.* 2008, *23*, 157–164.

[5] Norazalina, S., Norhaizan, M. E., Hairuszah, I., Norashareena, M. S., Anticarcinogenic efficacy of phytic acid extracted from rice bran on azoxymethane-induced colon carcinogenesis in rats. *Exp. Toxicol. Pathol.* 2010, *62*, 259–268.

[6] El-Sherbiny, Y. M., Cox, M. C., Ismail, Z. A., Shamsuddin, A. M., Vucenik, I., G0/G1 arrest and S phase inhibition of human cancer cell lines by inositol hexaphosphate (IP6). *Anticancer Res.* 2001, *21*, 2393–2403.

[7] Ferry, S., Matsuda, M., Yoshida, H., Hirata, M., Inositol hexakisphosphate blocks tumor cell growth by activating apoptotic machinery as well as by inhibiting the Akt/NFkappaB-mediated cell survival pathway. *Carcinogenesis* 2002, *23*, 2031–2041.

[8] Sandberg, A. S., Andersson, H., Effect of dietary phytase on the digestion of phytate in the stomach and small intestine of humans. *J. Nutr.* 1988, *118*, 469–473.

[9] Rapp, C., Lantzsch, H. J., Drochner, W., Hydrolysis of phytic acid by intrinsic plant and supplemented microbial phytase (*Aspergillus niger*) in the stomach and small intestine of minipigs fitted with re-entrant cannulas. 3. Hydrolysis of phytic acid (IP6) and occurrence of hydrolysis products (IP5, IP4, IP3 and IP2). *J. Anim. Physiol. Anim. Nutr.* 2001, *85*, 420–430.

[10] Cruickshank, E. W., Duckworth, J., Kosterlitz, H. W., Warnock, G. M., The digestibility of the phytic acid of oatmeal in adult man. *J. Physiol.* 1945, *104*, 41–46.

[11] Wise, A., Gilburt, D. J., Phytate hydrolysis by germfree and conventional rats. *Appl. Environ. Microbiol.* 1982, *43*, 753–756.

[12] Suzuki, T., Nishioka, T., Ishizuka, S., Hara, H., A novel mechanism underlying biological actions of phytate - Phytate hydrolysates induce intracellular calcium signaling by a Gαq protein coupled receptor- and phospholipase C-dependent mechanism in colorectal cancer cells. *Mol. Nutr. Food Res.* 2010 DOI: 10.1002/mnfr.200900279.

[13] Feigin, M. E., Muthuswamy, S. K., Polarity proteins regulate mammalian cell–cell junctions and cancer pathogenesis. *Curr. Opin. Cell Biol.* 2009, *21*, 694–700.

[14] Owaribe, K., Kodama, R., Eguchi, G., Demonstration of contractility of circumferential actin bundles and its morphogenetic significance in pigmented epithelium *in vitro* and *in vivo*. *J. Cell Biol.* 1981, *90*, 507–514.

[15] Yonemura, S., Itoh, M., Nagafuchi, A., Tsukita, S., Cell-to-cell adherens junction formation and actin filament organization: similarities and differences between non-polarized fibroblasts and polarized epithelial cells. *J. Cell. Sci.* 1995, *108*, 127–142.

[16] Krendel, M., Gloushankova, N. A., Bonder, E. M., Feder, H. H. *et al.*, Myosin-dependent contractile activity of the actin cytoskeleton modulates the spatial organization of cell–cell contacts in cultured epitheliocytes. *Proc. Natl. Acad. Sci. USA* 1999, *96*, 9666–9670.

[17] Krendel, M. F., Bonder, E. M., Analysis of actin filament bundle dynamics during contact formation in live epithelial cells. *Cell. Motil. Cytoskeleton* 1999, *43*, 296–309.

[18] Suzuki, T., Hara, H., Quercetin enhances intestinal barrier function through the assembly of zonula occludens-2, occludin, and claudin-1 and the expression of claudin-4 in Caco-2 cells. *J. Nutr.* 2009, *139*, 965–974.

[19] Laemmli, U. K., Cleavage of structural proteins during the assembly of the head of bacteriophage T4. *Nature* 1970, *227*, 680–685.

[20] Kamm, K. E., Stull, J. T., The function of myosin and myosin light chain kinase phosphorylation in smooth muscle. *Annu. Rev. Pharmacol. Toxicol.* 1985, *25*, 593–620.

[21] Amano, M., Ito, M., Kimura, K., Fukata, Y. *et al.*, Phosphorylation and activation of myosin by Rho-associated kinase (Rho-kinase). *J. Biol. Chem.* 1996, *271*, 20246–20249.

[22] Nakamura, M., Tokunaga, F., Sakata, S., Iwai, K., Mutual regulation of conventional protein kinase C and a ubiquitin ligase complex. *Biochem. Biophys. Res. Commun.* 2006, *351*, 340–347.

[23] Brodie, C., Blumberg, P. M., Regulation of cell apoptosis by protein kinase c delta. *Apoptosis* 2003, *8*, 19–27.

[24] Vucenik, I., Ramakrishna, G., Tantivejkul, K., Anderson, L. M., Ramljak, D., Inositol hexaphosphate (IP6) blocks proliferation of human breast cancer cells through a PKCdelta-dependent increase in p27Kip1 and decrease in retinoblastoma protein (pRb) phosphorylation. *Breast Cancer Res. Treat.* 2005, *91*, 35–45.

[25] Owen, R. W., Weisgerber, U. M., Spiegelhalder, B., Bartsch, H., Faecal phytic acid and its relation to other putative markers of risk for colorectal cancer. *Gut* 1996, *38*, 591–597.

[26] Ferguson, E. L., Gibson, R. S., Thompson, L. U., Ounpuu, S., Dietary calcium, phytate, and zinc intakes and the calcium, phytate, and zinc molar ratios of the diets of a selected group of East African children. *Am. J. Clin. Nutr.* 1989, *50*, 1450–1456.

[27] Ma, G., Li, Y., Jin, Y., Zhai, F. *et al.*, Phytate intake and molar ratios of phytate to zinc, iron and calcium in the diets of people in China. *Eur. J. Clin. Nutr.* 2007, *61*, 368–374.

[28] Ellis, R., Kelsay, J. L., Reynolds, R. D., Morris, E. R. *et al.*, Phytate:zinc and phytate X calcium:zinc millimolar ratios in self-selected diets of Americans, Asian Indians, and Nepalese. *J. Am. Diet. Assoc.* 1987, *87*, 1043–1047.

